JPET Fast Forward. Published on April 1, 2009 as DOI: 10.1124/jpet.109.151225

JPET #151225

Title page

Differential regulation of receptor activation and agonist selectivity by highly conserved tryptophans in the nicotinic acetylcholine receptor binding site

Dustin K. Williams, Clare Stokes, Nicole A. Horenstein, and Roger L. Papke*

Department of Pharmacology and Therapeutics, University of Florida College of Medicine, Gainesville, Florida (DKW, CS, & RLP)

Department of Chemistry, University of Florida, Gainesville, Florida (NAH)

JPET #151225

Running title page

Running title: Regulation of nAChR activation and agonist selectivity

*To whom correspondence should be addressed:
Name: Roger L. Papke
Phone: 352-392-4712
Fax: 352-392-9696
E-mail: rlpapke@ufl.edu
Address: Department of Pharmacology and Therapeutics
University of Florida
P.O. Box 100267
Gainesville, FL 32610-0267

Number of text pages: 28
Number of tables: 1
Number of figures: 9
Number of references: 37
Number of words in Abstract: 250
Number of words in Introduction: 700
Number of words in Discussion: 1500

Abbreviations:
nAChR, nicotinic acetylcholine receptor; ACh, acetylcholine; 4OH-GTS-21, 3-(4-hydroxy,2-methoxybenzylidene)anabaseine; LBD, ligand-binding domain; AChBP, acetylcholine binding protein; AR-R17779, (-)-Spiro[1-azabicyclo(2.2.2)octane-3,5′-oxazolidin-2′-one]; PNU-120596, 1-(5-chloro-2,4-dimethoxy-phenyl)-3-(5-methyl-isoxanol-3-yl)-urea; A, alanine; F, phenylalanine; G, glycine; V, valine; W, tryptophan; Y, tyrosine; R, arginine; S, serine; T, threonine

Abstract:

We have previously shown that a highly conserved tyrosine (Y) in the nicotinic acetylcholine receptor (nAChR) ligand-binding domain (LBD) (α7Y188 or α4Y195) differentially regulates the activity of acetylcholine (ACh) and the α7-selective agonist 3-(4-hydroxy,2-methoxybenzylidene)anabaseine (4OH-GTS-21) in α4β2 and α7 nAChR. In this study we mutated two highly conserved LBD tryptophan (W) residues in human α7 and α4β2 and expressed the receptors in *Xenopus* oocytes. Alpha7 receptors with W55 mutated to G (glycine) or Y became less responsive to 4OH-GTS-21, while mutation of the homologous W57 in β2 to G, Y, phenylalanine (F), or alanine (A) resulted in α4β2 receptors which showed increased responses to 4OH-GTS-21. Mutation of α7W55 to valine (V) resulted in receptors for which the partial agonist 4OH-GTS-21 became equally efficacious as ACh, while α4β2 receptors with the homologous mutation remained non-responsive to 4OH-GTS-21. In contrast to the striking alterations in agonist activity profiles that were observed with mutations of α7W55 and β2W57, mutations of α7W149 or α4W154 universally resulted in receptors with reduced function. Our data support the hypothesis that some conserved residues in the nAChR LBD differentially regulate receptor activation by subtype-selective agonists, while other, equally well-conserved residues play fundamental roles in receptor activation by any agonist. Residues like α7W149 (α4W154) may be considered pillars upon which basic receptor function depends, while α7W55 (β2W57) and α7Y188 (α4Y195) may be fulcra upon which agonists may operate differentially in specific receptor subtypes, consistent with the hypothesis that ACh and 4OH-GTS-21 are able to activate nAChR in distinct ways.

Introduction:

The Cys-loop superfamily of ligand-gated ion channels, which includes channels gated by acetylcholine (ACh), serotonin, gamma-aminobutyric acid, and glycine (G), have been hypothesized to have evolved from a common ancestor (Ortells and Lunt, 1995). Sequence analysis of receptor subunits within the Cys-loop superfamily, all the way through to prokaryotic ligand-gated ion channels, illustrate remarkable conservation at select sites and have implicated great functional significance to aromatic residues localized in the ligand-binding domain (LBD) of receptors within the Cys-loop superfamily (Tasneem et al., 2005). In nicotinic acetylcholine receptors (nAChR), tryptophan (W) 55 and W149 (α7 numbering) have been identified amongst other aromatic ring-containing residues as highly conserved throughout evolution and as contributors to the formation of a hydrophobic LBD (Cohen et al., 1991; Tomaselli et al., 1991; Devillers-Thiery et al., 1993; Aylwin and White, 1994; Galzi and Changeux, 1995; Chiara and Cohen, 1997; Chiara et al., 1998; Brejc et al., 2001; Xiu et al., 2009).

Several studies have shown that mutation of highly conserved aromatic residues typically results in decreased efficacy and/or potency for ACh and related ammonium compounds (Galzi et al., 1991; O'Leary and White, 1992; Sine et al., 1994; Xie and Cohen, 2001). However, observations by Horenstein et al. (2006) suggest that mutation of conserved aromatic residues may not result in loss of receptor activity for all ligands, and conserved aromatic residues may differentially regulate receptor activation by select agonists. Specifically, the activation of human α7 nAChR by 3-(4-hydroxy,2-methoxybenzylidene)anabaseine (4OH-GTS-21), an α7-selective agonist, is unaffected by mutation of tyrosine (Y) 188 to phenylalanine (F), while ACh potency is drastically reduced in the mutant α7 receptor. The effect of the homologous mutation was qualitatively different in heteromeric α4β2 receptors. While ACh potency was unaffected by the α4Y195F (previously reported as α4Y190F) mutation, the efficacy of 4OH-GTS-21 was increased at least 200-fold in α4Y195Fβ2 receptors relative to wild type (Horenstein et al., 2006). These findings suggest that the assumption that all conserved residues play comparable roles in all receptor subtypes may be invalid and have led us to hypothesize that other conserved residues within the aromatic pocket may

JPET Fast Forward. Published on April 1, 2009 as DOI: 10.1124/jpet.109.151225
This article has not been copyedited and formatted. The final version may differ from this version.

act as metaphorical pivots or fulcrums which confer unique pharmacological properties to different receptor subtypes rather than as structural pillars, which play universal roles in all receptors in which they are conserved.

Seventeen known genes (α1-10, β1-4, δ, γ, and ε) are translated into membrane-spanning proteins that may form nAChR subunits and can assemble into a large variety of pentameric complexes which display distinct pharmacology, physiologic localization, and functionality (Dani and Bertrand, 2007). The LBD is localized at the interface of two subunits; W55 and W149 (α7 numbering) are found on opposing sides of this interface. In heteromeric receptors such as α4β2 and muscle-type receptors, W57 is found on the non-α subunit (complementary face) while W154 (α4 numbering) is found on the α subunit (primary face) contributing to the binding site. As might be expected, the only subunits in which α7W55 and β2W57 are not conserved are subunits which do not form the complementary face, while the only subunits in which α7W149 and α4W154 are not conserved are subunits which do not contribute to the primary face of an agonist binding site (Figure 1A). These tryptophans are both found in α subunits which can form homomeric receptors (α7 - α10) since these α subunits contribute to both the primary and complementary faces of binding sites in the homomeric receptor (Kalamida et al., 2007). The crystal structure of acetylcholine binding protein (AChBP) isolated from *Lymnaea stagnalis*, which is homologous to the extracellular domain of a homomeric receptor (Brejc et al., 2001), suggests that the indole ring of the W at position 149 (human α7 numbering) is positioned vertically, deeper, and slightly higher in the binding pocket than W55, which is positioned horizontally at the mouth of the aromatic pocket (Figure 1B).

In this study we use site-directed mutagenesis and heterologous expression in *Xenopus* oocytes to investigate the functional significance of α4W154, β2W57, α7W55, and α7W149 for the activation of homomeric and heteromeric neuronal nAChR by ACh and the structurally diverse α7-selective agonists choline, 4OH-GTS-21, and (-)-Spiro[1-azabicyclo(2.2.2)octane-3,5′ -oxazolidin-2′ -one] (AR-R17779). Our data suggest that nAChR are likely activated in different manners by structurally distinct agonists and provide insight regarding the selective activation of nAChR subtypes.

Methods:

cDNA clones

Human nAChR receptor clones were obtained from Dr. Jon Lindstrom (University of Pennsylvania, Philadelphia PA). The RIC-3 clone was obtained from Dr. Millet Treinin (Hebrew University, Jerusalem Israel).

Site-directed Mutants

Mutations of selected amino acids were introduced using the QuikChange kit from Stratagene (La Jolla CA) according to the manufacturer's instructions. Sequences were confirmed with automated fluorescent sequencing at the University of Florida core facility.

Preparation of RNA

Subsequent to linearization and purification of cloned cDNAs, RNA transcripts were prepared in vitro using the appropriate mMessage mMachine kit from Ambion Inc. (Austin TX).

Expression in Xenopus laevis oocytes

Mature (>9 cm) female *Xenopus laevis* African frogs (Nasco, Ft. Atkinson WI) were used as a source of oocytes. Before surgery the frogs were anesthetized by placing them in a 1.5 g/l solution of MS222 for 30 min. Oocytes were removed from an incision made in the abdomen.

Harvested oocytes were treated with 1.25 mg/ml collagenase (Worthington Biochemical Corporation, Freehold NJ) for two hours at room temperature in calcium-free Barth's solution (88 mM NaCl, 1 mM KCl, 2.38 mM $NaHCO_3$, 0.82 mM $MgSO_4$, 15 mM HEPES (pH 7.6), 12 mg/l tetracycline) in order to remove the follicular layer. Stage-5 oocytes were isolated and injected with 50 nl (5-20 ng) of each subunit cRNA. Recordings were normally conducted 2-5 days post-injection, although for some mutants longer periods of incubation (up to 8-10 days) were required to obtain measurable currents. Wild-type and mutant α7 receptors were routinely co-injected with the cDNA for human RIC-3, an accessory protein that improves and accelerates α7 expression (Halevi et al., 2003) without affecting the pharmacological properties of the receptors. Alpha4β2 receptors were injected at an α:β ratio of 1:1. Note that the injection of α4 and

JPET Fast Forward. Published on April 1, 2009 as DOI: 10.1124/jpet.109.151225
This article has not been copyedited and formatted. The final version may differ from this version.

β2 subunits into the oocytes at a ratio of 1:1 results in a mixture of $(\alpha4)_2(\beta2)_3$ and $(\alpha4)_3(\beta2)_2$ stoichiometries (Kuryatov et al., 2008).

Electrophysiology

Experiments were conducted using OpusXpress6000A (Molecular Devices, Union City CA). OpusXpress is an integrated system that provides automated impalement and voltage clamp of up to eight oocytes in parallel. Both the voltage and current electrodes were filled with 3M KCl. The oocytes were clamped at a holding potential of -60 mV. Data were collected at 50 Hz and filtered at 20 Hz. The oocytes were bath-perfused with Ringer's solution (115mM NaCl, 2.5mM KCl, 1.8mM $CaCl_2$, 10mM HEPES, 1μM atropine, pH 7.2). Agonist solutions were delivered from a 96-well plate using disposable tips. Flow rates were set at 2 ml/min for α7 and 4 ml/min for α4β2. Drug applications were 12 s for α7 and 6 s for α4β2 and usually alternated between ACh controls and test solutions of ACh or other experimental agonists at varying concentrations.

Chemicals

4OH-GTS-21 was obtained from Taiho (Tokyo, Japan). AR-R17779 was provided by Critical Therapeutics, Inc. (Lexington MA). Other chemicals were purchased from Sigma. Fresh acetylcholine stock solutions were made daily in Ringer's solution.

Molecular Modeling and Sequence Alignment

The molecular graphic of AChBP (Figure 1B, 1i9B; (Brejc et al., 2001)) was produced using the UCSF Chimera package from the Resource for Biocomputing, Visualization, and Informatics at the University of California, San Francisco (Pettersen et al., 2004). Sequence alignments were generated using ClustalW at www.ebi.ac.uk/Tools/clustalw2/index.html (Higgins et al., 1996). Homology modeling (Figure 8) utilized the Swiss-Model Server at *http://swissmodel*.expasy.org (Schwede et al., 2003; Kopp and Schwede, 2004; Arnold et al., 2006). Briefly, the template for both human α7 and α4β2 nAChR dimer models was the crystal structure for AChBP in complex with cocaine (2PGZ; (Hansen and Taylor, 2007)). Cocaine has previously been shown to be a core structure that can be modified to form the α7-selective partial agonist cocaine methiodide (Francis et al., 2001). The 2PGZ structure was chosen because the

binding of cocaine positions the C-loop in a way that is consistent with the accommodation of α7-selective agonists that are bulkier than ACh, such as cocaine methiodide, tropanes, quinuclidines, and benzylidene anabaseine compounds. Note that 2PGZ is the wild-type AChBP structure, containing the C-loop disulfide and all other conserved elements of the LBD. ClustalW sequence alignments were used between the AChBP sequence and either human α7, α4, or β2 nAChR sequences. The resulting monomer models were then fit to the coordinates of an AChBP dimer to produce $\alpha7_2$, and α4β2 dimer models. Side chains experiencing clashes at the interface were identified and optimized using side-chain conformational searching and the GROMOS96 force field within the Swiss-PDBviewer (version 4.01). Modeling of 4OH-GTS-21 bound in the LBD of α7 or α4β2 models was performed with DOCK6.1 (Moustakas et al., 2006).

Experimental protocols and data analysis

Responses of α4β2 wild-type and mutant receptors are reported as peak currents, and responses of α7 wild-type and mutant receptors are calculated as net-charge (Papke and Papke, 2002) since peak currents inaccurately report the agonist concentration dependence of α7-mediated responses (Papke and Thinschmidt, 1998).

Comparison of functional expression between mutant and wild-type receptors

ACh-induced maximum responses for mutant receptors compared to wild-type receptors (Figures 3A, 3C, 6A, and 7A) were calculated by averaging responses to the same concentration of ACh on both wild-type and mutant receptors on the same day, using the same batch of oocytes which had been injected with equal amounts of RNA on the same day. Such precautions are necessary to accurately determine maximal responses relative to wild-type receptors due to biological variability inherent within oocytes harvested from different frogs. For example, differences in the mediators of metabolic processes (kinases, phosphatases, cyclic nucleotides, etc) and/or hormonal regulation between individual frogs could affect rates of protein synthesis or intracellular signaling cascades leading to varied phosphorylation states among the expressed receptors. ACh tests were 300 μM for α7 wildtype and α7W55 mutants. Alpha7W55Y was also tested with 30 μM ACh, and the nonresponsive mutants α7W55S and α7W55T were also tested with 3 mM ACh. ACh tests were 100 μM and 1 mM for α4β2 wildtype and

α4β2W57 mutants. ACh tests were 300 μM and 1 mM for α7 wildtype and α7W149 mutants, and 30 μM and 1mM for α4β2 wildtype and α4W154β2 mutants. Four - 18 oocytes were tested from each group, with on average n=7. The test ACh responses were then normalized to the expected ACh maximum for each receptor type as determined by full ACh concentration response studies done separately.

Concentration-Response Relationships

Each oocyte received two initial control applications of ACh followed by the experimental drug application and a subsequent control application of ACh. For experiments with α7 wild-type and mutant receptors, the control ACh concentration was 300 μM; except 30 μM ACh was used as the control for α7W55Y because this mutant could not be activated repeatedly by 300 μM ACh without rundown, hypothetically due to accumulated desensitization; and choline and ACh curves for α7W55G were done using 1 mM ACh as a control because results were overly variable when 300 μM ACh was used as the control, presumably due to the low potency of ACh for this mutant. For experiments with α4β2 wild-type receptors and α4β2W57 mutants control applications of ACh were 30 μM, and for experiments with α4W149β2 mutants control ACh applications were 100 μM ACh. Responses to experimental drug applications were calculated relative to the preceding ACh control responses in order to normalize the data, compensating for the varying levels of channel expression among the oocytes, and were subsequently normalized to the ACh maximum response for each receptor type, determined from separate ACh concentration-response experiments.

Mean values and standard errors (SEM) were calculated from the normalized responses of at least four oocytes (average 7) for each experimental concentration. For concentration-response relations, data were plotted using Kaleidagraph 3.52 (Synergy Software, Reading PA), and curves were generated from the Hill equation: Response = $(I_{max}[agonist]^n)/([agonist]^n + (EC_{50})^n)$, where I_{max} denotes the maximal response for a particular agonist/subunit combination, and n represents the Hill coefficient. I_{max}, n, and the EC_{50} were all unconstrained for the fitting procedures except in the case of the ACh concentration-response curves. Because ACh is our reference full agonist, those data were normalized to the observed ACh maximum, and the I_{max} of the curve fits were

constrained to equal 1. Although some α4β2 concentration-response curves were not ideally fit by the single-site Hill equation, presumably because α4β2 receptors expressed from RNA injected at a α4:β2 ratio of 1:1 resulted in α4β2 receptors of mixed stoichiometry (Kuryatov et al., 2008), in most cases the single-site Hill equation provided better concentration-response curve fits than the double-site Hill equation, and so for consistency, single-site fits were generated for all α4β2 data sets.

Results:

Mutation of W55 or W57 of α7 and α4β2 receptors, respectively, alters the pharmacology and regulates the selectivity of 4OH-GTS-21.

We anticipated two general types of effects that would result from mutations in the nAChR LBD: firstly that there would be changes in the ability of ACh to promote channel activation, secondly that there would be differences in the relative efficacy of α7-selective agonists compared to ACh.

Since our primary goal was to test the hypothesis that α7-selective agonists may promote activation through mechanisms that are distinct from the activation mechanism invoked by ACh, changes in relative efficacy were of particular interest. While measurements of relative efficacy are readily obtainable from macroscopic currents as long as a reliable reference by which to measure efficacy is employed, effects of the first type, on the absolute ability of ACh to promote activation, are relatively difficult to measure from macroscopic currents since decreases in ACh-evoked responses may result from either decreased ACh activity or decreased receptor expression. An obstacle in this study for the application of traditional measurements of receptor expression, such as radioligand binding assays, is that mutations of highly conserved LBD residues are arguably equally likely to affect ligand binding as receptor activation, potentially rendering results of binding experiments uninterpretable.

Absolute efficacy of ACh: With this limitation in mind, we estimated the effects of our mutations on the absolute effectiveness of ACh to promote channel activation based on comparisons of the maximum ACh-induced currents in our mutants to the maximum ACh-induced currents in wild-type receptors that were injected the same day from the same harvest of oocytes with RNA of comparable amount and quality, as confirmed on denaturing gels, in combination with concentration-response curves for

ACh. The estimates should be accurate to the degree that the LBD mutation had a greater effect on ACh activation than on net receptor expression. These measurements of maximal ACh-induced currents then formed the basis from which efficacies of choline, 4OH-GTS-21, and AR-R17779, relative to ACh responses in wild-type and mutant receptors, were subsequently determined. Choline and AR-R17779 are considered full agonists of α7, activating α7 as efficaciously as ACh, while 4OH-GTS-21 is an α7-selective partial agonist. None of these drugs produce significant currents in α4β2 receptors (Figure 2).

Calculated ACh maximum responses for α7W55A and α7W55G mutants were approximately 2.5 times larger than for wild-type, the α7W55 to valine (V) mutant maximum responses were approximately equal to wild-type, and α7W55Y and α7W55F had ACh maximum net-charge responses approximately one half as large as wild-type α7 (Figure 3A). It has previously been reported (Gay et al 2008), that the W55A mutant of rat α7 showed a reduced decay rate in macroscopic currents, which might account for our observed increase in net charge compared to wild-type α7. However, our data indicate that, similar to wild-type α7, the human W55A and W55G mutants show typical concentration-dependent desensitization, such that the net charge of the ACh responses reach a maximal value at relatively low concentrations of agonist, while peak currents show a higher apparent EC_{50} (not shown).

Homologous mutations were made in β2; wild-type and β2 mutant subunits were co-expressed (1:1) with α4. As with the α7W55 mutants, the α4β2W57A, G, V, Y, and F mutants gave functional responses to ACh, and α4β2W57 arginine (R), serine (S), and threonine (T) mutants did not (Figure 3B and D). However, none of the α4β2 mutant peak currents were as large as the wild-type responses. The calculated maximum ACh responses of the functional mutants were on average approximately one tenth of the wild-type calculated maximum ACh peak response (Figure 3C). Nonetheless, the ACh potencies were greater for some of the α4β2W57 mutants than for the wild-type (see Figure 5).

Relative efficacy of α7-selective agonists compared to ACh: The mutation of α7W55 to the non-aromatic amino acids A, G, and V resulted in reduced potencies for all

the agonists tested (Figure 4A-C, Table 1). Although mutation of α7W55 to G produced a decrease in the potency of ACh, choline, and AR-R17779 (22-fold, 14-fold, and >92-fold increases in EC_{50} values, respectively, Table 1), maximal responses to these agonists were larger than those of wild-type receptors. Maximal ACh responses of α7W55G mutants were about 2.5 fold higher than maximal ACh responses in wild-type receptors. Relative to the maximum ACh-induced currents in wild-type and mutant receptors choline efficacy was increased (Figure 4B). While the 10 mM choline responses were significantly larger than the 1 mM ACh responses recorded in the same cells ($n = 10$, $p < 0.05$), due to the low potency of choline for the W55G mutant, we were unable to achieve a saturating I_{max} for choline in the concentration range tested (up to 10 mM). In contrast to the results seen with ACh and choline, α7W55G receptors did not produce measurable responses to 4OH-GTS-21 in the concentration range tested. Mutation of α7W55 to A or V likewise resulted in decreased agonist potencies, although not as greatly as with the mutation to G (Figure 4A and C, Table 1). 4OH-GTS-21 activated the α7W55V mutant as efficaciously as ACh (Figure 4C). The relatively conservative mutation of W55 to Y or F did not significantly affect ACh potency, as EC_{50} values remained near 30 μM. However, the potencies of choline, 4OH-GTS-21, and AR-R17779 were all altered by these mutations (Table 1). Mutation of W55 to F caused the EC_{50} of 4OH-GTS-21 to increase 6-fold (Figure 4D) and mutation of W55 to Y yielded mutant α7 receptors that did not give detectable responses to 4OH-GTS-21.

The low efficacy of 4OH-GTS-21 for the W55G and W55Y α7 mutants seems to be, at least in part, related to desensitization and/or channel block by 4OH-GTS-21. When 100 μM 4OH-GTS-21 was co-applied with ACh to the W55G and W55Y mutant receptors, responses were significantly decreased compared to responses to ACh applied alone ($p < 0.05$, data not shown). We have previously characterized a similar type of residual inhibition/desensitization (RID) in wild-type α7 receptors (Papke et al., 2009) and have shown that it can represent a form of stabilized desensitization that is reversed by the application of the Type 2 positive allosteric modulator PNU-120596 (1-(5-chloro-2,4-dimethoxy-phenyl)-3-(5-methyl-isoxanol-3-yl)-urea.). Although 4OH-GTS-21 was relatively ineffective at activating α7 W55G and W55Y mutant receptors, large currents

occurred when 4OH-GTS-21 was applied with PNU-120596 (not shown). These observations suggest that 4OH-GTS-21 has access to the binding site in the α7 W55 mutants, and promotes PNU-120596-sensitive desensitization much more effectively than activation.

Homologous mutations in the LBD of α4β2 receptors (β2W57) produced qualitatively different results from the mutations made in α7. Mutation to G greatly reduced ACh potency in α7 receptors, but increased ACh potency in α4β2W57G mutants. Mutation of W55 to Y in α7 receptors did not affect ACh potency, but ACh was twice as potent for α4β2W57Y mutants as for wild-type receptors. ACh also had greater potency for α4β2W57F than for wild-type α4β2. However, ACh had significantly lower potency for α4β2W57A than for wild-type α4β2. Neither choline nor AR-R17779 activated any of the α4β2 receptors (Figure 5A-E, Table 1). However, 4OH-GTS-21 did activate four of the α4β2W57 mutants and provided the most interesting differences amongst these W55 and W57 mutants of the α7-selective agonists tested. Note that maximal ACh responses of the α4β2 mutants were approximately one-tenth of the maximal responses in wild-type receptors. While it is true that a selective compromise in ACh-mediated activation would have the tendency to make the relative efficacies of the experimental agonists appear increased, that effect would be manifested in the results of all experimental agonists normalized to the ACh responses. However, our data indicate that the increase in the relative efficacy of 4OH-GTS-21 is many times larger than that of either choline or AR-R17779, which were both immeasurable because currents induced by these drugs were too small to be determined. Therefore, the increased activation of α4β2 mutants by 4OH-GTS-21 is likely to represent a true potentiation of an activation mechanism potentially unique to 4OH-GTS-21 and related compounds. 4OH-GTS-21 activated wild-type α4β2 only about 2% and wild-type α7 46% as well as ACh (Figure 2B-C). 4OH-GTS-21 activated α4β2W57A, G, F and Y, but not α4β2W57V, R, S, or T mutant receptors. Interestingly, 4OH-GTS-21 activated α7W55V mutants as well as ACh did. 4OH-GTS-21 activated α4β2W57A, F, and G to 60-70% of their ACh maxima, with lowest potency in α4β2W57A and highest potency in α4β2W57Y and α4β2W57F mutants. Importantly, peak responses of α4β2W57Y to

JPET Fast Forward. Published on April 1, 2009 as DOI: 10.1124/jpet.109.151225
This article has not been copyedited and formatted. The final version may differ from this version.

4OH-GTS-21 were 2.5-fold greater than for ACh, while the homologous mutation in α7 decreased the relative efficacy of 4OH-GTS-21 greatly.

Mutation of W149 in both α7 and α4β2 receptors reduced receptor activation by both ACh and α7-selective agonists.

Responses of α7W149 mutant receptors were significantly lower ($p < 0.05$) than those of wild-type α7 receptors recorded the same number of days post-injection. Somewhat surprisingly, the relatively conservative mutations of α7W149 to F or Y disrupted receptor responses to ACh to levels below the limits of detection, while the non-conservative mutations to A or G yielded receptors that were capable of producing measurable ACh-induced currents. The α7W149V mutant receptors were also non-responsive to ACh (Figure 6A). Of the mutant receptors that were non-responsive to ACh, none were able to produce recordable currents in response to choline, 4OH-GTS-21, or AR-R17779, with the exception of α7W149F mutants, which reproducibly yielded small but measurable currents in response to choline (not shown). The fact that only two of the five α7W149 mutants were sufficiently functional for use in this study suggests that mutation introduced at position 149 may interfere with receptor assembly or with conformational changes linked to channel opening. The mutations introduced at position 149 in α7 resulted in drastically reduced potencies of ACh, choline, and AR-R17779 (Table 1). Mutation of α7W149 to G had profound effects on receptor activation, resulting in 13-, 20-, and 140-fold increases in EC_{50} values over those seen in wild-type receptors for ACh, choline, and AR-R17779, respectively. However, neither α7W149A nor α7W149G mutant receptors had significantly altered potency for 4OH-GTS-21 compared to wild type. Compared to the maximum response of ACh in wild-type receptors, the efficacy of choline fell 30% and the efficacy of 4OH-GTS-21 rose 50% in α7W149G mutants (Figure 6C-D, Table 1).

Alpha4W154β2 mutant receptors produced measurable ACh-induced currents when mutations to A, F or W were introduced, while currents were undetectable when G was introduced at position 149, roughly the opposite of what was observed in α7W149 mutants (Figure 7A-B). This observation is suggestive of intrinsic differences between the α7 and α4β2 LBDs. There was no functional expression of α4W154Gβ2 or

α4W154Vβ2 mutant receptors detected; these mutants were also non-responsive to choline, 4OH-GTS-21, and AR-R17779 (not shown).

Mutation of α4W154 to A resulted in a 7-fold increase in the EC_{50} for ACh, while mutations to F or Y did not greatly alter ACh potency compared to wild type. Of the α4W154β2 mutants tested, none responded to choline, AR-R17779, or 4OH-GTS-21 (Figure 7C-E).

In general, a loss of receptor function was observed as a result of any mutation introduced at the W149 position, at least for the agonists we tested and mutations we introduced. Taken together, these results suggest the W55 position may better tolerate mutation than W149, and when mutated allows for major alterations in the receptor activation mechanisms, especially in regard to choline and 4OH-GTS-21.

Homology modeling of the α7 and α4β2 ligand binding domains with 4OH-GTS-21.

Figure 8 presents views of 4OH-GTS-21 docked in the LBD of the human α7 and α4β2 receptors based on homology modeling. The viewer's perspective is from the extracellular side of the receptor, with the C loop and the cysteine disulfide in the lower left. Docking 4OH-GTS-21 into either the α7 or α4β2 receptor model produced very similar poses for the compound-receptor complex. One difference between these complexes is that W149 and W55 are in close communication in the α7 model, but are not in the heteromeric receptor. The indole ring of W55 has a "flipped" conformation in the α4β2 model relative to the α7 model because the initially obtained model suffered from non-covalent interactions that were relieved by rotating the W57 β-γ bond by approximately 180 degrees prior to minimization. Another key difference observed between the poses for the two receptors was that docking 4OH-GTS-21 into the α4β2 receptor model resulted in a twist of the benzylidine double bond by approximately 50 degrees, an unreasonable amount. None of the other low energy poses identified placed the 4OH-GTS-21 in a similar location within the LBD.

Discussion:

Numerous mutational studies of α7W55 and α7W149 (and homologous residues in other nAChR subtypes) and other conserved aromatic residues within the aromatic box of the nAChR LBD generally lead one to believe that mutation of conserved aromatic

residues results in reduced receptor functionality. Building on evidence from a previous study, which showed that mutation of α7Y188 does not necessarily knock down receptor functionality for all agonists, we investigated the functional significance of the conserved α7W55, β2W57, α7W149, and α4W154 residues.

Using unnatural amino acid substitutions in muscle-type nAChR at positions αW86, αW149, αW184, γW55/δW57 with W derivatives containing various degrees of predicted cation interaction energies, αW149 has been shown to establish primary interactions with the quaternary ammonium group of acetylcholine (Zhong et al., 1998; Xiu et al., 2009). Structures of AChBP reveal either a charged nitrogen poised over the indole ring or hydrogen bonding interactions with ligands and the AChBP W143, homologous to human α7W149 (Brejc et al., 2001; Celie et al., 2004; Hansen et al., 2005). Another implication of the data from Zhong *et al*. was that W55 may not directly stabilize the quaternary group of ACh through cation-π interactions, and the specific role of this residue in receptor activation remains an open question. In *Torpedo* receptors, mutation of γW55 to leucine (L) reduced ACh affinity 7,000-fold, while similar mutation of δW57 resulted in only a 20-fold reduction. Double-mutant receptors (γW55L and δW57L) were reported to have reduced binding of many small agonists, including tetramethylammonium. Nicotine binding, however, was unaffected by the double-mutant receptors (Xie and Cohen, 2001). W55 was recently proposed to affect desensitization kinetics (Gay et al., 2008). However, results of this study are inconclusive since α7 currents were measured as peak responses (Papke and Papke, 2002), mutation of W55 affected agonist potency which in turn alters the response waveform (Papke, 2006), and macroscopic currents alone are insufficient to determine kinetics of desensitization.

Our data suggest that the conserved residues W149 and W55 have different functional significance in α7 nAChR, behaving as a pillar or as a fulcrum, respectively (Figure 9). We apply the fulcrum metaphor to W55 and Y188 (α7 numbering) since mutation of these amino acids provides ligand and/or subtype-dependent changes in channel activation. While the α7-agonist 4OH-GTS-21 lost efficacy in α7W55 mutants relative to ACh, the same agonist gained efficacy, up to 300-fold compared to ACh in some α4β2W57 and α4Y195Fβ2 mutants. The data from the current study suggest that

W55 may be a critical residue for how 4OH-GTS-21 can either activate or fail to activate the gating mechanism. Perhaps the same ligand-residue interactions exist in both α7 and α4β2 nAChR subtypes but with different effects on activation, or perhaps the homologous residues form different ligand-residue interactions depending on the receptor subtype. For example, cation-π interactions may be formed in one subtype while the –NH group on the indole ring of W may donate a hydrogen bond in the alternate subtype. In the model of 4OH-GTS-21 docked in the LBD of wild-type α4β2, W55 is localized in such a position that its bulkiness appears to be a primary cause for forcing an unreasonable twist of the benzylidene group's double bond (Figure 8). If compounds like 4OH-GTS-21 bind with the benzylidine group in a position similar to that modeled, the mutation of W55/W57 may significantly alter ligand-receptor interactions on the complementary face in a receptor subtype-dependent fashion. The observation that α4β2 receptors gain function with 4OH-GTS-21 when W57 is mutated to smaller residues is consistent with the idea that the wild-type receptor has unfavorable steric clashes with this compound. In the case of the α7 receptor, the interactions of 4OH-GTS-21 with W55 may be optimum, such that in general, making this position smaller in size results in less favorable binding and/or function. The increase in 4OH-GTS-21 efficacy observed in W55V mutants may result from the beta branching of V, which confers sufficient size that receptor function is maintained or, in this case, potentiated relative to ACh responses.

The possibility that 4OH-GTS-21 is capable of interacting with nicotinic receptors in unique ways to induce receptor activation cannot be ruled out, suggesting a given ligand may have multiple alternative binding conformations. In one receptor subtype the conformations that can catalyze gating may be favored over alternative conformations that do not. Mutations such as the β2W57Y may alter the preferred binding of 4OH-GTS-21 and increasing probability that gating will occur. In the current study, 4OH-GTS-21 is the only agonist we tested which efficaciously activated certain α4β2 mutants while losing α7 efficacy. Likewise, in the previous study with Y188F mutants, anabaseine derivatives were the only α7 agonists tested that activated the mutant α4β2 receptors, with 4OH-GTS-21 being the most efficacious by far (Horenstein et al., 2006). These observations raise questions regarding how 4OH-GTS-21 activates the nAChR. While it

is possible that 4OH-GTS-21 may fit into the binding site of wild-type α7 and α4β2 in different conformations, it is also likely that ligands such as ACh and 4OH-GTS-21 form different types of intermolecular interactions with residues in the protein, and thereby promote receptor activation in different ways. Investigations of AChBP bound with agonists and antagonists have led to the idea that channel opening and, possibly, ligand selectivity may occur through a conformation induced by the ligand which is due to the inherent flexibility of the binding site, allowing it to conform to the structural characteristics of the ligand (Hansen et al., 2005). A potentially important observation is that acetylcholine, choline, and AR-R17779 all contain sp^3 hybridized ammonium nitrogen atoms, and hence the onium substituent groups occupy space in three dimensions. The onium nitrogen atom thought to be important in 4OH-GTS-21 binding is sp^2 hybridized and flat, resulting in a lower steric demand. This difference in three-dimensional structure between choline, AR-R17779 and 4OH-GTS-21 may underlie some of the unique observations made in this study regarding 4OH-GTS-21. Work is in progress to further explore this hypothesis via homology modeling and comparative docking studies of these alternate agonists

In contrast to the variable effects of W55 mutations, W149 seems to serve more like a structural "pillar" in the LBD (Figure 9), universally important for receptor function, regardless of agonist or receptor subtype. However, if W149 were solely responsible for stabilizing the ligand, one would expect to see total loss of receptor activity when this residue became incapable of forming cation-π interactions. Clearly this was not the case as non-aromatic α7 W149 mutant receptors still responded to agonists, and mutation to other aromatic residues actually produced receptors that were non-responsive to ACh. Other aromatic residues and non-aromatic residues found within the LBD probably help to stabilize and compensate for lost interactions resulting from mutation, or perhaps form an alternate set of interactions with ACh that are still capable of activating the receptor when the W149 is mutated. As shown in Figure 8, the LBD places three electron-rich Y residues around the cationic ammonium center. These groups may compensate for the mutation of W149 in regard to cation recognition, in the W149 mutants that were functional. One general observation that may be made from the homology modeling is that the conserved W149 is placed in an ideal position to impact

JPET Fast Forward. Published on April 1, 2009 as DOI: 10.1124/jpet.109.151225
This article has not been copyedited and formatted. The final version may differ from this version.

receptor structure and function because it effectively lines the LBD pocket under the C-loop, providing a large hydrophobic face to this pocket. Mutations here may have a general deleterious effect because they disrupt this core part of the LBD. If the fulcrum-and-pillar hypothesis is correct, residues localized in the vicinity of the LBD may establish interactions with the ligand that place it in a position in which its ability to interact with the receptor and initiate changes in channel gating is regulated by conserved amino acids such as W55 or Y188 (α7 numbering). Identification of other residues that may contribute to the ability of conserved residues to regulate receptor activation by subtype-selective agonists is an important topic of future research.

Adding insight to the results presented here is the report that serotonin activates the highly homologous mouse 5-HT_3 and *C. elegans* MOD-1 receptors through formation of cation-π interactions at different W residues, at the position homologous to W149 in $5HT_3$ and at the position homologous to Y195 in MOD-1. In MOD-1 the residues at the positions homologous to 149 and 195 in α7 are Y and W, respectively (Mu et al., 2003). Mutation of these residues suggested that both receptors make specific contacts with serotonin that regulate channel gating, but those specific contacts depend on the nature of the binding site. Evolutionary pressures may have allowed some flexibility in the ability of conserved aromatic residues to act differentially in different receptors, or serotonin may be accommodating to the distinct binding domains, finding alternate ways to establish interactions that lead to receptor activation.

In conclusion, our data augment the existing evidence that structurally distinct agonists are capable of activating receptors in unique ways and provide new details regarding possible mechanisms of α7-selective nAChR activation and agonist selectivity.

Acknowledgments:

We thank Lisa Jacobs, Lynda Cortes, Sara Braley, and Shehd Al Rubaiy for technical assistance.

References:

Arnold K, Bordoli L, Kopp J and Schwede T (2006) The SWISS-MODEL workspace: a web-based environment for protein structure homology modelling. *Bioinformatics* **22**:195-201.

Aylwin ML and White MM (1994) Ligand-receptor interactions in the nicotinic acetylcholine receptor probed using multiple substitutions at conserved tyrosines on the alpha subunit. *FEBS Lett* **349**:99-103.

Brejc K, van Dijk WJ, Klaassen RV, Schuurmans M, van Der Oost J, Smit AB and Sixma TK (2001) Crystal structure of an ACh-binding protein reveals the ligand-binding domain of nicotinic receptors. *Nature* **411**:269-276.

Celie PH, van Rossum-Fikkert SE, van Dijk WJ, Brejc K, Smit AB and Sixma TK (2004) Nicotine and carbamylcholine binding to nicotinic acetylcholine receptors as studied in AChBP crystal structures. *Neuron* **41**:907-914.

Chiara DC and Cohen JB (1997) Identification of amino acids contributing to high and low affinity d-tubocurarine sites in the Torpedo nicotinic acetylcholine receptor. *J Biol Chem* **272**:32940-32950.

Chiara DC, Middleton RE and Cohen JB (1998) Identification of tryptophan 55 as the primary site of [3H]nicotine photoincorporation in the gamma-subunit of the Torpedo nicotinic acetylcholine receptor. *FEBS Lett* **423**:223-226.

Cohen JB, Sharp SD and Liu WS (1991) Structure of the agonist-binding site of the nicotinic acetylcholine receptor. [3H]acetylcholine mustard identifies residues in the cation-binding subsite. *J Biol Chem* **266**:23354-23364.

Dani JA and Bertrand D (2007) Nicotinic acetylcholine receptors and nicotinic cholinergic mechanisms of the central nervous system. *Annu Rev Pharmacol Toxicol* **47**:699-729.

Devillers-Thiery A, Galzi JL, Eisele JL, Bertrand S, Bertrand D and Changeux JP (1993) Functional architecture of the nicotinic acetylcholine receptor: a prototype of ligand-gated ion channels. *J Membr Biol* **136**:97-112.

Francis MM, Cheng EY, Weiland GA and Oswald RE (2001) Specific activation of the alpha 7 nicotinic acetylcholine receptor by a quaternary analog of cocaine. *Mol Pharmacol* **60**:71-79.

Galzi JL, Bertrand D, Devillers-Thiery A, Revah F, Bertrand S and Changeux JP (1991) Functional significance of aromatic amino acids from three peptide loops of the alpha 7 neuronal nicotinic receptor site investigated by site-directed mutagenesis. *FEBS Lett* **294**:198-202.

Galzi JL and Changeux JP (1995) Neuronal nicotinic receptors: molecular organization and regulations. *Neuropharmacology* **34**:563-582.

Gay EA, Giniatullin R, Skorinkin A and Yakel JL (2008) Aromatic residues at position 55 of rat alpha7 nicotinic acetylcholine receptors are critical for maintaining rapid desensitization. *J Physiol* **586**:1105-1115.

Gotti C, Zoli M and Clementi F (2006) Brain nicotinic acetylcholine receptors: native subtypes and their relevance. *Trends Pharmacol Sci* **27**:482-491.

Halevi S, Yassin L, Eshel M, Sala F, Sala S, Criado M and Treinin M (2003) Conservation within the RIC-3 gene family. Effectors of mammalian nicotinic acetylcholine receptor expression. *J Biol Chem* **278**:34411-34417.

Hansen SB, Sulzenbacher G, Huxford T, Marchot P, Taylor P and Bourne Y (2005) Structures of Aplysia AChBP complexes with nicotinic agonists and antagonists reveal distinctive binding interfaces and conformations. *Embo J* **24**:3635-3646.

Hansen SB and Taylor P (2007) Galanthamine and non-competitive inhibitor binding to ACh-binding protein: evidence for a binding site on non-alpha-subunit interfaces of heteromeric neuronal nicotinic receptors. *J Mol Biol* **369**:895-901.

Higgins DG, Thompson JD and Gibson TJ (1996) Using CLUSTAL for multiple sequence alignments. *Methods Enzymol* **266**:383-402.

Horenstein NA, McCormack TJ, Stokes C, Ren K and Papke RL (2006) Reversal of agonist selectivity by mutations of conserved amino acids in the binding site of nicotinic acetylcholine receptors. *J Biol Chem* **282**:5899-5909.

Kalamida D, Poulas K, Avramopoulou V, Fostieri E, Lagoumintzis G, Lazaridis K, Sideri A, Zouridakis M and Tzartos SJ (2007) Muscle and neuronal nicotinic acetylcholine receptors. Structure, function and pathogenicity. *Febs J* **274**:3799-3845.

Kopp J and Schwede T (2004) The SWISS-MODEL Repository of annotated three-dimensional protein structure homology models. *Nucleic Acids Res* **32**:D230-234.

Kuryatov A, Onksen J and Lindstrom J (2008) Roles of accessory subunits in alpha4beta2(*) nicotinic receptors. *Mol Pharmacol* **74**:132-143.

Moustakas DT, Lang PT, Pegg S, Pettersen E, Kuntz ID, Brooijmans N and Rizzo RC (2006) Development and validation of a modular, extensible docking program: DOCK 5. *J Comput Aided Mol Des.* **20**:601-619.

Mu TW, Lester HA and Dougherty DA (2003) Different binding orientations for the same agonist at homologous receptors: a lock and key or a simple wedge? *J Am Chem Soc* **125**:6850-6851.

O'Leary ME and White MM (1992) Mutational analysis of ligand-induced activation of the Torpedo acetylcholine receptor. *J Biol Chem* **267**:8360-8365.

Ortells MO and Lunt GG (1995) Evolutionary history of the ligand-gated ion-channel superfamily of receptors. *Trends Neurosci* **18**:121-127.

Papke RL (2006) Estimation of both the potency and efficacy of alpha7 nAChR agonists from single-concentration responses. *Life Sci* **78**:2812-2819.

Papke RL and Papke JKP (2002) Comparative pharmacology of rat and human alpha7 nAChR conducted with net charge analysis. *Br J of Pharm* **137**:49-61.

Papke RL and Thinschmidt JS (1998) The correction of alpha7 nicotinic acetylcholine receptor concentration-response relationships in *Xenopus* oocytes. *Neurosci. Let.* **256**:163-166.

Pettersen EF, Goddard TD, Huang CC, Couch GS, Greenblatt DM, Meng EC and Ferrin TE (2004) UCSF Chimera--a visualization system for exploratory research and analysis. *J Comput Chem* **25**:1605-1612.

Schwede T, Kopp J, Guex N and Peitsch MC (2003) SWISS-MODEL: An automated protein homology-modeling server. *Nucleic Acids Res* **31**:3381-3385.

Sine SM, Quiram P, Papanikolaou F, Kreienkamp HJ and Taylor P (1994) Conserved tyrosines in the alpha subunit of the nicotinic acetylcholine receptor stabilize quaternary ammonium groups of agonists and curariform antagonists. *J Biol Chem* **269**:8808-8816.

Tasneem A, Iyer LM, Jakobsson E and Aravind L (2005) Identification of the prokaryotic ligand-gated ion channels and their implications for the mechanisms and origins of animal Cys-loop ion channels. *Genome Biol* **6**:R4.

Tomaselli GF, McLaughlin JT, Jurman ME, Hawrot E and Yellen G (1991) Mutations affecting the agonist sensitivity of the nicotinic acetylcholine receptor. *Biophys. J.* **60**:721-727.

Xie Y and Cohen JB (2001) Contributions of Torpedo nicotinic acetylcholine receptor gamma Trp-55 and delta Trp-57 to agonist and competitive antagonist function. *J Biol Chem* **276**:2417-2426.

Xiu X, Puskar NL, Shanata JA, Lester HA and Dougherty DA (2009) Nicotine binding to brain receptors requires a strong cation-pi interaction. *Nature.*

Zhong W, Gallivan JP, Zhang Y, Li L, Lester HA and Dougherty DA (1998) From ab initio quantum mechanics to molecular neurobiology: a cation-pi binding site in the nicotinic receptor. *Proc Natl Acad Sci U S A* **95**:12088-12093.

Footnotes:

These studies were supported by a grant from the National Institute of Health [GM57481].

Legends for Figures

Figure 1. Multiple sequence alignment and hypothetical localization of α4W154, β2W57, α7W55, and α7W149. **A)** Multiple sequence alignment of human nAChR sequences with sample sequences from chick, *C. elegans*, and zebrafish show great conservation of both W residues throughout the nicotinic family and many species. Unc-38 and unc-20 from *C. elegans* encode α and non-α subunits, respectively (source: www.wormbase.org). Curiously, these Ws are also conserved in the α5 and β3 subunits, which have been proposed to occupy the accessory subunit position and not contribute directly to the agonist binding domain (Gotti et al., 2006). **B)** Closeup of the LBD from the crystal structure of AChBP isolated from *L. stagnalis* (PDB ID: 1i9b). Numbering of residues correspond to human α7 numbering.

Figure 2. Concentration-response relationships of wild-type α7 and α4β2 receptors to ACh, choline, 4OH-GTS-21, and AR-R17779. **A)** Chemical structures of the agonists used in this study. **B)** Net-charge responses of wild-type α7. **C)** Peak responses of wild-type α4β2. Each data point represents the mean (±SEM) of at least four oocytes. For consistency the single-site Hill equation was used to fit the α4β2 curve since the single-site model provided the best fit for most α4β2 mutants in this study. There were no significant differences in chi square or R values between fits by the single-site or biphasic models.

Figure 3. Functional responses of human α7W55 and human α4β2W57 mutant receptors relative to ACh-induced maximum responses in wild-type. **A)** Maximum net-charge responses of α7W55 mutant receptors relative to the ACh-induced maximum net-charge response in wild-type α7, represented as a value of 1. * and ** denote statistically significant differences in maximal functional responses between wild-type and mutant receptors with $p<0.05$ and $p<0.01$, respectively. **B)** Representative data traces of responses by α7 wild-type and α7W55 mutants to 300μM ACh. **C)** Maximum peak responses of α4β2W57 mutants relative to the ACh-induced maximum peak response in

wild-type α4β2, represented as a value of 1. * and ** denote $p<0.05$ and $p<0.01$, respectively. **D)** Representative data traces of α4β2W57 mutant receptors in response to 30 μM ACh. Maximum responses for mutant receptors compared to wild type were calculated by averaging responses (± SEM) of at least four oocytes to the same concentration of ACh on both wild-type and mutant receptors injected the same day, with the same amount of RNA from the same harvest of oocytes. Averaged responses were divided by the percent of ACh maximum for that concentration on a fitted ACh concentration-response curve to find the maximum theoretical response, and then divided by the calculated maximum response for the wild-type receptor for the comparison.

Figure 4. Concentration-response relationship of α7W55 mutant receptors to ACh, choline, 4OH-GTS-21, and AR-R17779. **A)** Net-charge responses of α7W55A mutants. **B)** Net-charge responses of α7W55G mutants. Note the low efficacy of 4OH-GTS-21. **C)** Net-charge responses of α7W55V mutants. **D)** Net-charge responses of α7W55F mutants. **E)** Net-charge responses of α7W55Y mutants. Note the low efficacy of 4OH-GTS-21. Responses of wild-type α7 are presented in Figure 2B. Data were measured relative to control ACh responses and then expressed relative to the maximum ACh response for each particular receptor type. Each point represents the mean (±SEM) of at least four oocytes.

Figure 5. Concentration-response relationships of α4β2W57 mutants to ACh, choline, 4OH-GTS-21, and AR-R17779. **A)** Peak responses of α4β2W57A mutant receptors. **B)** Peak responses of α4β2W57G mutant receptors. **C)** Peak responses of α4β2W57V mutant receptors. **D)** Peak responses of α4β2W57F mutant receptors. **E)** Peak responses of α4β2W57Y mutant receptors. Note that α4β2W57A, α4β2W57G, α4β2W57F, and α4β2W57Y mutants responded to 4OH-GTS-21. Responses to choline and AR-R17779 were below the limits of detection of all α4β2 receptors. Data were measured relative to control ACh responses and then expressed relative to the maximum ACh response for each particular receptor type. Each point represents the mean (±SEM) of at least four oocytes. Peak responses by wild-type α4β2 are presented in Figure 2C.

Figure 6. Concentration-response relationships of α7W149 mutants to ACh, choline, 4OH-GTS-21, and AR-R17779. **A)** Maximum ACh-induced net-charge responses of α7W149 mutants compared to maximum net-charge response of ACh in wild-type α7. ** denotes $p<0.01$. **B)** Representative data traces of α7W149 mutants in response to 300 μM ACh. **C)** Net-charge responses of α7W149A mutant receptors. **D)** Net-charge responses of α7W149G mutant receptors. Each data point represents the mean (±SEM) of at least four oocytes. Responses of wild-type α7 to these agonists are presented in Figure 2B.

Figure 7. Concentration-response relationships of α4W154β2 mutants to ACh, choline, 4OH-GTS-21, and AR-R17779. **A)** Maximum ACh-induced peak responses of α7W149 mutants compared to the maximum peak response of ACh in wild-type α7. ** denotes $p<0.01$. **B)** Representative data traces of α4W154β2 mutants in response to 30 μM ACh. **C)** Peak responses of α4W154Aβ2 mutants. **D)** Peak responses of α4W154Fβ2 mutants. **E)** Peak responses of α4W154Aβ2 mutants. Each data point represents the mean (±SEM) of at least four oocytes. Peak responses by wild-type α4β2 are represented in Figure 2C.

Figure 8. LBDs for α7 and α4β2 nAChR homology models. **A)** The top panel presents the α7 structure with the best pose obtained for docking the agonist 4OH-GTS-21 into the LBD. The two key tryptophan residues, W149 and W55, are labeled. **B)** The bottom panel presents the α4β2 structure with a similar pose for the competitive antagonist 4OH-GTS-21, obtained by DOCK6.1 calculation.

Figure 9. Conserved residues in the nAChR LBD function as pillars or fulcrums. The W149 of α7 and the homologous residue in α4 are of critical importance for activation of both subtypes by ACh, and in α7, for activation by the subtype selective agonists tested: choline (Ch), 4OH-GTS-21 (BA), and AR-R17779 (AR). The down arrows represent the reduced activation observed with all of the W149 mutants tested. Grayed arrows represent responses to subtype-selective agonists that were reduced below the level of

detection. Horizontal arrows represent responses that were unchanged by mutations, and grayed horizontal arrows represent subthreshold responses below the limit of detection in both wildtype and mutant α4β2 receptors. In contrast, W55 of α7 and the homologous residue (W57) in β2 are critical determinants of the unique pharmacology of the α7 and α4β2 receptor subtypes. In α7 W55 appears to be important for activation by the subtype-selective agonists in balance with ACh. Mutations of W57 in β2 can make the receptors available for activation by 4OH-GTS-21 while at the same time reducing responses to ACh compared to wildtype. The boxes denote mutations which have opposite effects in α7 and α4β2.

JPET Fast Forward. Published on April 1, 2009 as DOI: 10.1124/jpet.109.151225
This article has not been copyedited and formatted. The final version may differ from this version.

Table 1: EC_{50} and I_{max} values of ACh, Choline, 4OH-GTS-21, and AR-R17779 in wild-type and mutant α7 and α4β2 receptors

Drug	Receptor	EC_{50} ± SEM	I_{max} ± SEM relative to ACh maximum	I_{max} ± SEM relative to wild-type ACh maximum
ACh	α7	31 ± 4	1	1
	α7W55A	85 ± 6	1	2.5 ± 0.4
	α7W55F	33 ± 3	1	0.5 ± 0.1
	α7W55G	602 ± 35	1	2.4 ± 0.25
	α7W55V	84 ± 2.5	1	1.2 ± 0.1
	α7W55Y[¥]	30 ± 5	1	0.6 ± 0.2
	α7W149A	194 ± 10	1	0.15 ± 0.03
	α7W149G	400 ± 19	1	0.17 ± 0.03
	α4β2	76 ± 20	1	1
	α4β2W57A	468 ± 59	1	0.09 ± 0.01
	α4β2W57F	33 ± 4	1	0.04 ± 0.02
	α4β2W57G	47 ± 11	1	0.08 ± 0.02
	α4β2W57V	87 ± 10	1	0.05 ± 0.013
	α4β2W57Y	16 ± 2	1	0.08 ± 0.03
	α4W154A β2	526 ± 28	1	0.40 ± 0.04
	α4W154F β2	118 ± 6	1	0.39 ± 0.06
	α4W154Y β2	81 ± 3	1	0.04 ± 0.00
Choline	α7	304 ± 21	0.90 ± 0.02	0.90 ± 0.02
	α7W55A	950 ± 210	0.95 ± 0.05	2.3 ± 0.1
	α7W55F	500 ± 72	1.4 ± 0.07	0.73 ± 0.04
	α7W55G	> 5,000	1.3± 0.12	> 1.5
	α7W55V	570 ± 12	1.1 ± 0.01	1.4 ± 0.1
	α7W55Y	228 ± 13	0.84 ± 0.01	0.48 ± 0.01
	α7W149A	2490 ± 130	0.89 ± 0.03	0.13 ± 0.01
	α7W149G	6870 ± 1440	0.61 ± 0.07	0.10 ± 0.02
4OH-GTS-21	α7	3.0 ± 0.3	0.46 ± 0.01	0.46 ± 0.01
	α7W55A	8.4 ± 0.7	0.33 ± 0.01	0.82 ± 0.02
	α7W55F	19 ± 2	0.45 ± 0.02	0.23 ± 0.01
	α7W55G	NA*	NA*	NA*
	α7W55V	7.8 ± 0.8	0.94 ± 0.03	0.54 ± 0.02
	α7W55Y	NA*	NA*	NA*
	α7W149A	4.5 ± 1.4	0.28 ± 0.04	0.04 ± 0.01
	α7W149G	4.4 ± 0.5	0.76 ± 0.08	0.13 ± 0.02
	α4β2	NA*	0.01 ± 0.00	0.01 ± 0.005
	α4β2W57A	2.6 ± 0.3	0.71 ± 0.02	0.07 ± 0.01
	α4β2W57F	0.66 ± 0.22	0.62 ± 0.05	0.02 ± 0.002
	α4β2W57G	1.2 ± 0.2	0.74 ± 0.04	0.06 ± 0.01
	α4β2W57V	3.00 ± 0.14	0.07 ± 0.01	0.0035 ± 0.0005
	α4β2W57Y	0.65 ± 0.09	2.7 ± 0.1	0.19 ± 0.01
AR-R17779	α7	3.60 ± 0.73	1.05 ± 0.05	1.05 ± 0.05
	α7W55A	32.4 ± 1.7	0.96 ± 0.02	2.36 ± 0.05
	α7W55F	82.3 ± 2.5	1.02 ± 0.01	0.53 ± 0.01
	α7W55G	332 ± 2	0.99 ± 0.04	2.36 ± 0.10
	α7W55V	94 ± 6	1.05 ± 0.04	1.26 ± 0.05
	α7W55Y	87 ± 42	0.90 ± 0.16	0.51 ± 0.09
	α7W149A	120 ± 4	1.07 ± 0.14	0.16 ± 0.02
	α7W149G	506 ± 72	0.97 ± 0.09	0.17 ± 0.02

[†] N values ranged from 4 to 18, and were on average 7.
*Responses were below the limits of detection.

A

	D Loop	B Loop
Q15822|ACHA2_HUMAN	EKNQMMTTNVWLKQEWSDYKLR	QQNCKMKFGSWTYDKAKIDLEQ
P32297|ACHA3_HUMAN	EVNQIMETNLWLKQIWNDYKLK	YQNCTMKFGSWSYDKAKIDLVL
P43681|ACHA4_HUMAN	EKNQMMTTNVWVKQEWHDYKLR	QQNCTMKFGSWTYDKAKIDLVN
P30532|ACHA5_HUMAN	EKNQLMTTNVWLKQEWIDVKLR	LQNCSMKFGSWTYDGSQVDIIL
Q15825|ACHA6_HUMAN	EVNQIMETNLWLRHIWNDYKLR	HQNCSLKFGSWTYDKAEIDLLI
P36544|ACHA7_HUMAN	EKNQVLTTNIWLQMSWTDHYLQ	VQHCKLKFGSWSYGGWSLDLQ-
Q9UGM1|ACHA9_HUMAN	ERNQILTAYLWIRQIWHDAYLT	NQQCNLTFGSWTYNGNQVDIFN
Q9GZZ6|ACH10_HUMAN	ERNQVLTLYLWIRQEWTDAYLR	AQHCGLTFGSWTHGGHQLDVRP
P17787|ACHB2_HUMAN	EREQIMTTNVWLTQEWEDYRLT	QQNCTMKFRSWTYDRTEIDLVL
Q05901|ACHB3_HUMAN	EKNQLMTTNVWLKQEWTDHKLR	RQNCSMKFGSWTYDGTMVDLIL
P30926|ACHB4_HUMAN	EREQIMTTNVWLKQEWTDYRLT	QQNCTLKFRSWTYDHTEIDMVL
Y00762|ACHA_HUMAN	EVNQIVTTNVRLKQQWVDYNLK	EQNCSMKLGTWTYDGSVVAINP
P11230|ACHB_HUMAN	EKDEEMSTKVYLDLEWTDYRLS	WQNCTMVFSSYSYDSSEVSLQT
Q07001|ACHD_HUMAN	EVEETLTTNVWIEHGWTDNRLK	WQNCSLKFSSLKYTAKEITLSL
Q04844|ACHE_HUMAN	EKEETLTTSVWIGIDWQDYRLN	WQNCSLIFRSQTYNAEEVEFTF
P07510|ACHG_HUMAN	EREEALTTNVWIEMQWCDYRLR	WQNCSLIFQSQTYSTNEIDLQL
P09482|ACHA4_CHICK	EKNQMMTTNVWVKQEWHDYKLR	QQNCKMKFGSWTYDKAKIDLVS
AJ250362|ACHB2_CHICK	EREQIMTTNVWLTQEWEDYRLT	QQNCTMKFRSWTYDRTEIDLVL
N957513|ACHA7_ZEBRAFISH	EKNQVLTTNIWLQLYWYDYYLQ	LQRCDLKFGSWTYGGWSLDLQ-
F21F3.5|unc-38_C.ELEGANS	EIDQIMTCSVWLKQTWIDRKLS	EQQCHLKFGSWTFSENLLSVEL
T08G11.5|unc-20_C.ELEGANS	EKDQVMHTNVWLTLQWHDFQMK	EQVCTLVFGSWTYNENEIKLEF
P58154|ACHBP_LYMST	EITNEVDVVFWQQTTWSDRTLA	-ATCRIKIGSWTHHSREISVDP

B

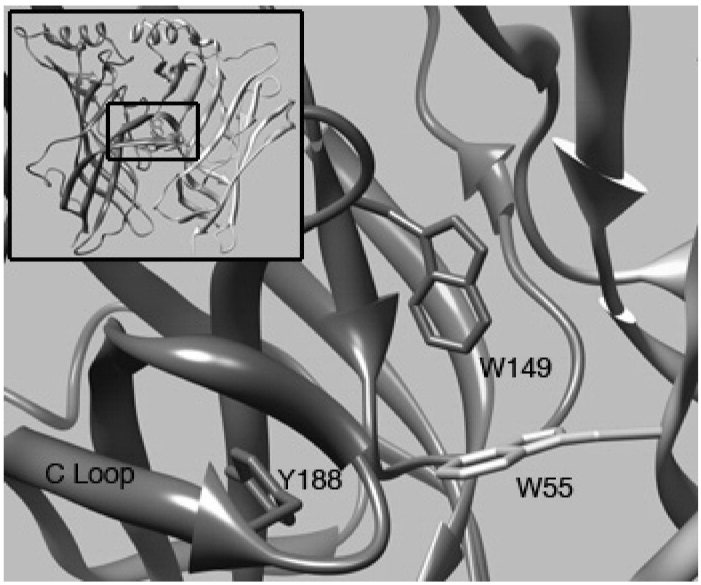

Figure 1

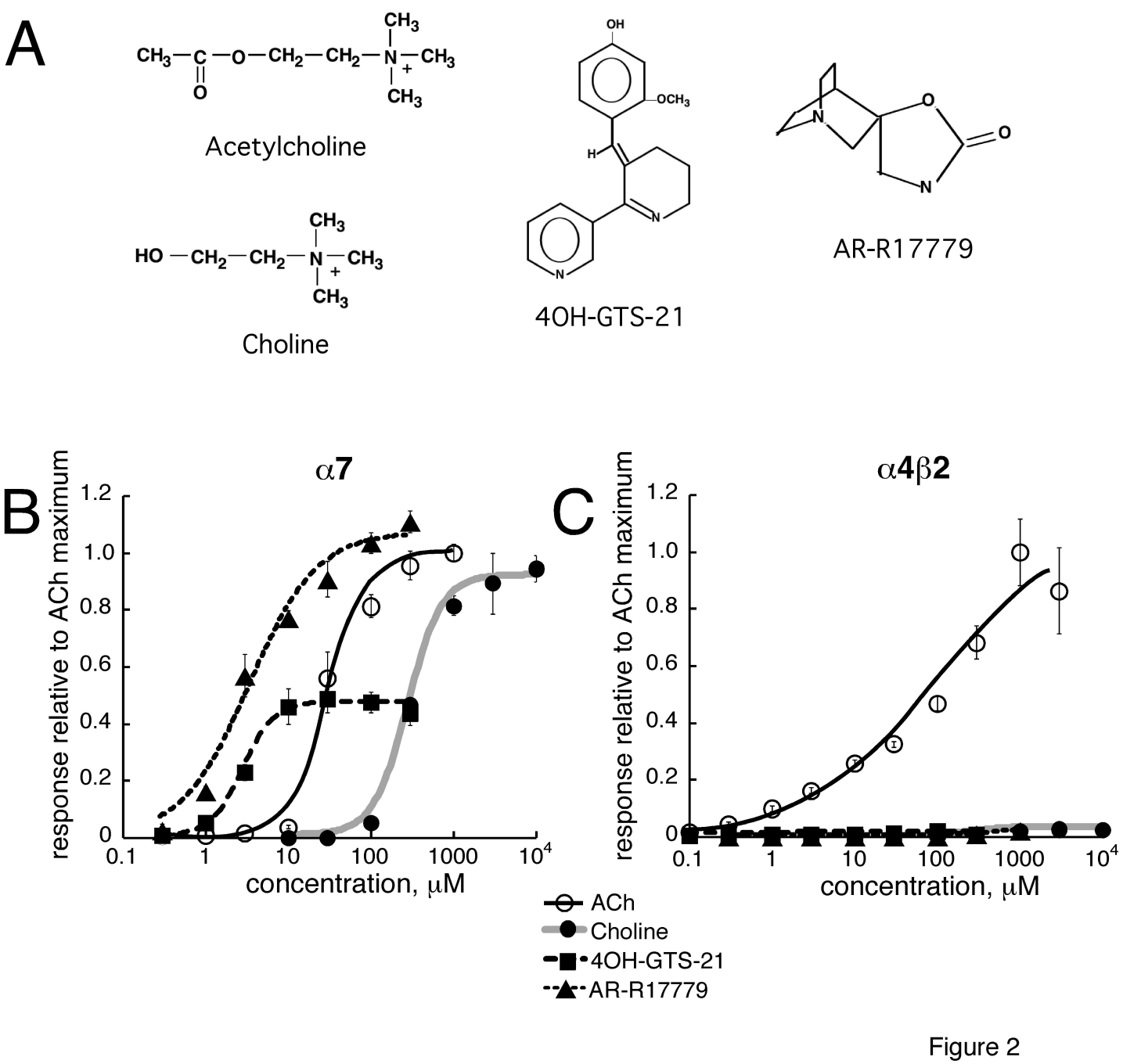
A
Acetylcholine
Choline
4OH-GTS-21
AR-R17779
B
α7
response relative to ACh maximum
concentration, μM
C
α4β2
response relative to ACh maximum
concentration, μM
ACh
Choline
4OH-GTS-21
AR-R17779

Figure 2

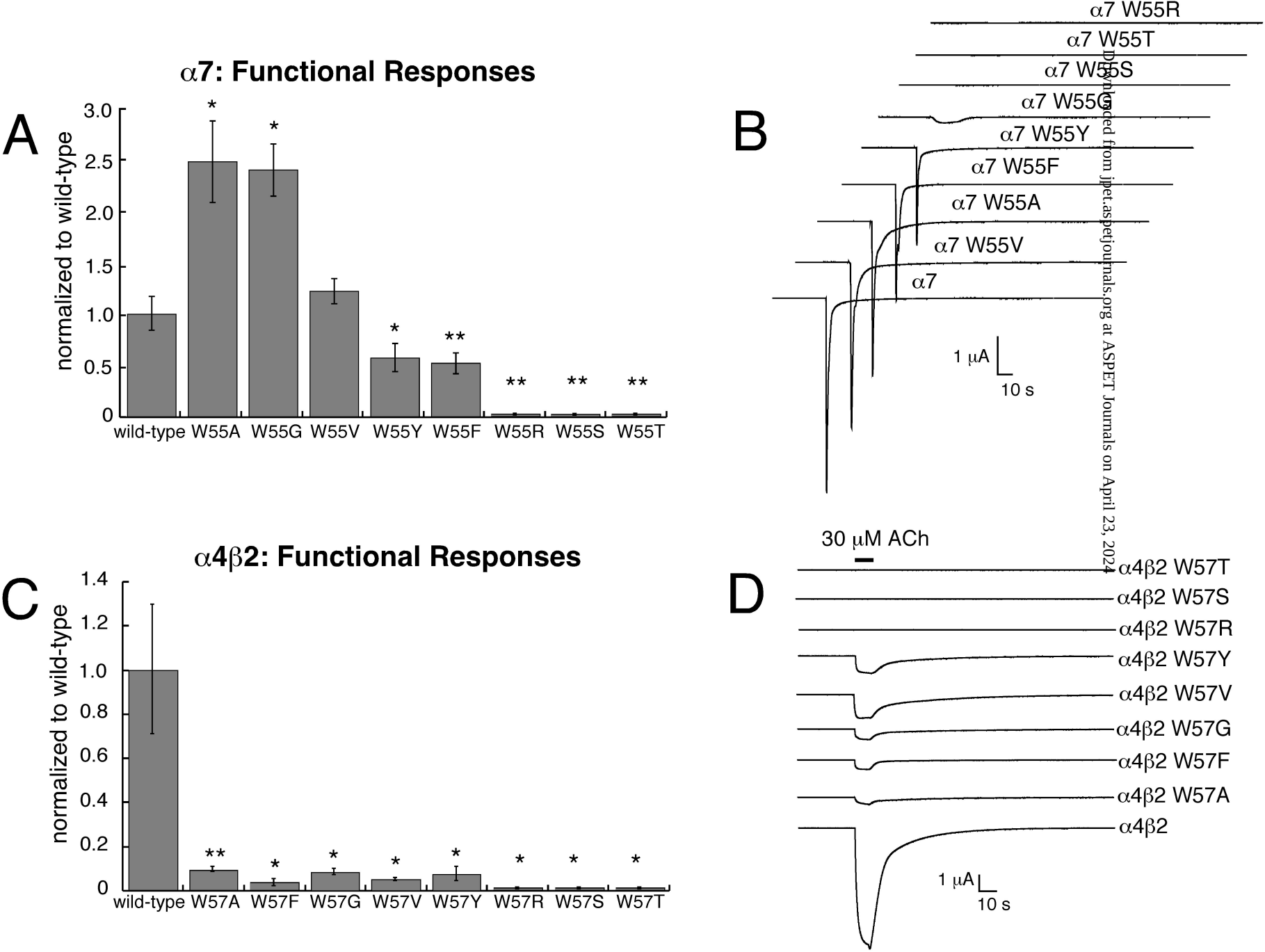

Figure 3

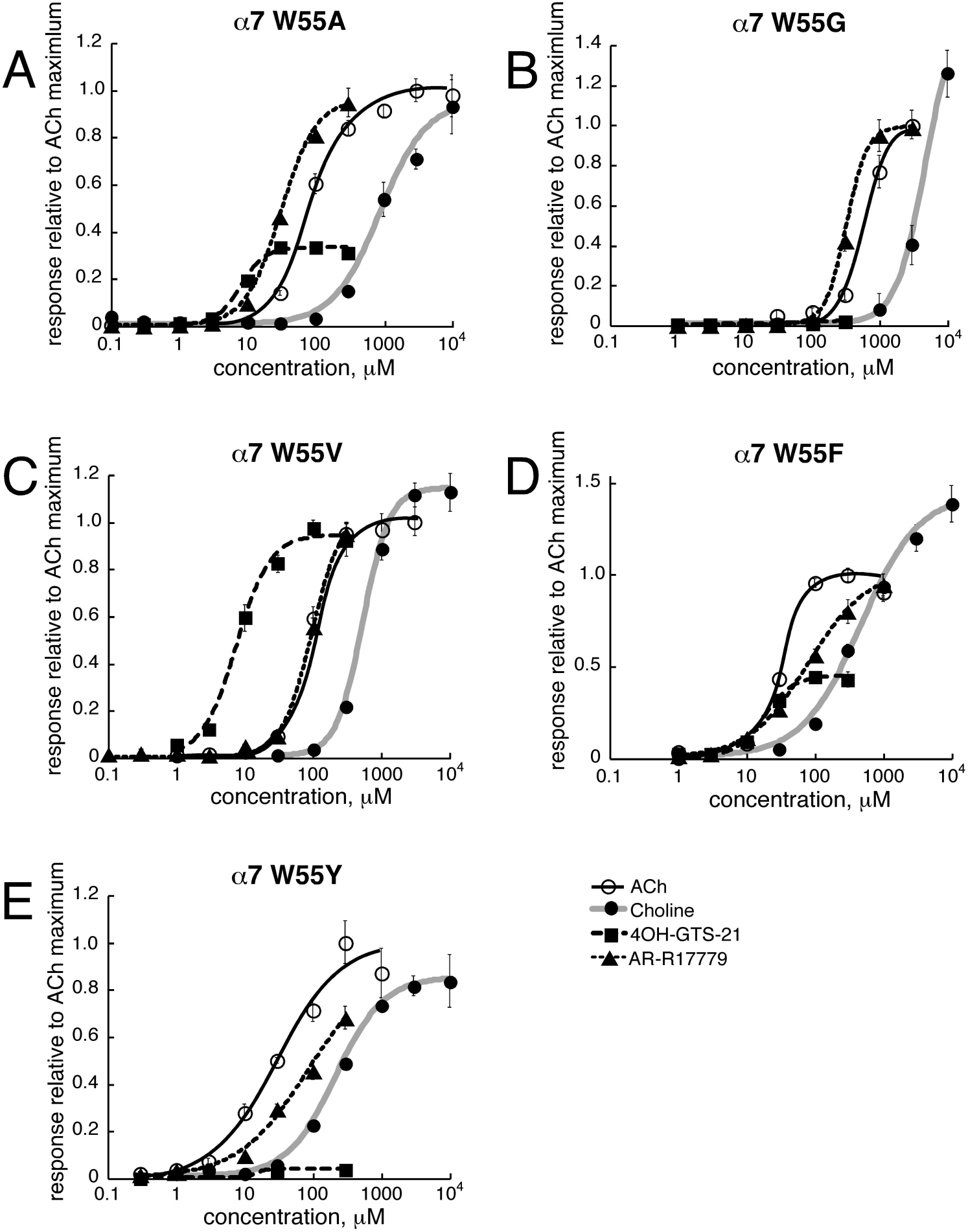
A
α7 W55A
response relative to ACh maximlum
concentration, μM
B
α7 W55G
response relative to ACh maximlum
concentration, μM
C
α7 W55V
response relative to ACh maximum
concentration, μM
D
α7 W55F
response relative to ACh maximum
concentration, μM
E
α7 W55Y
response relative to ACh maximum
concentration, μM
ACh
Choline
4OH-GTS-21
AR-R17779

Figure 4

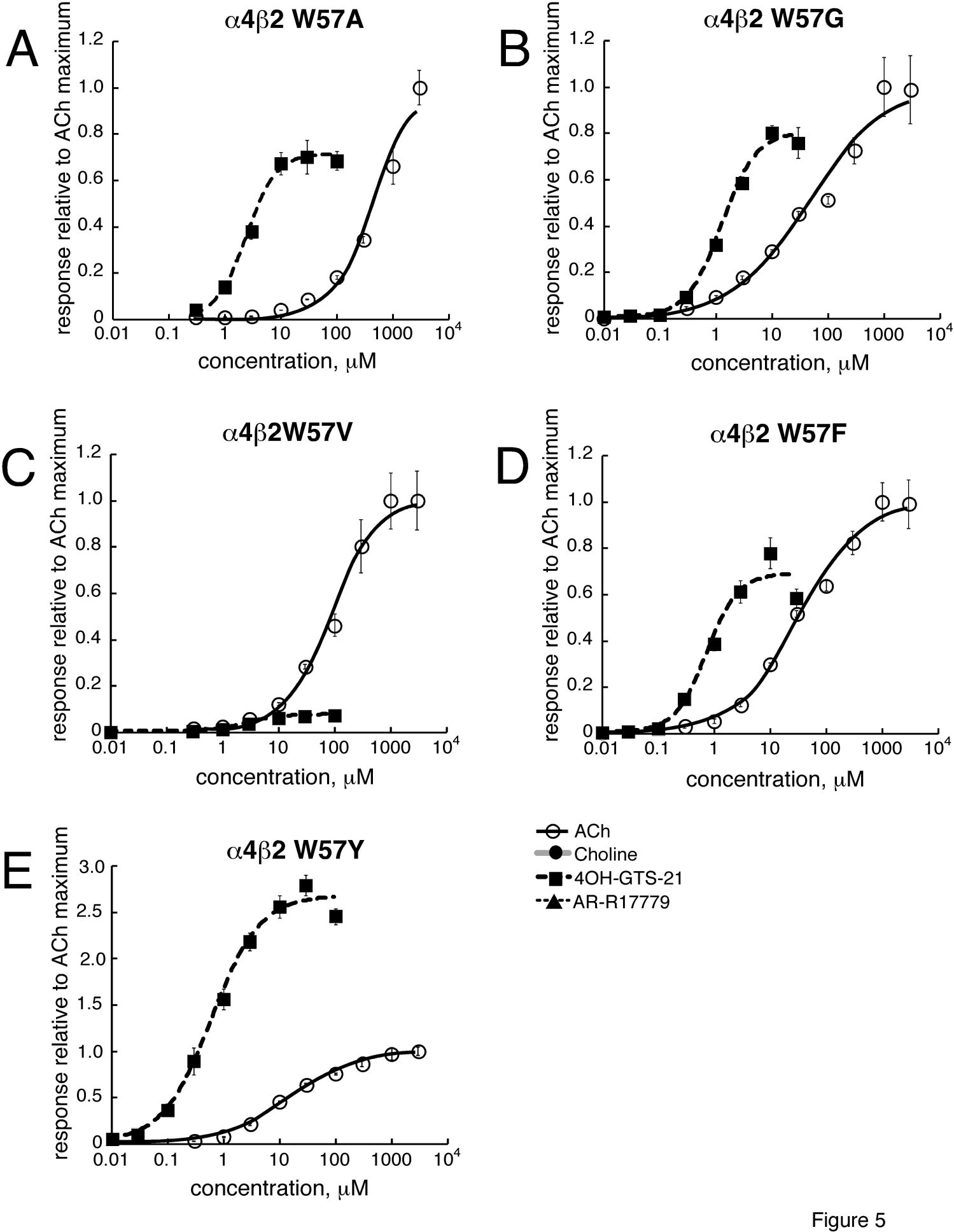
A
α4β2 W57A
response relative to ACh maximum
concentration, μM
B
α4β2 W57G
response relative to ACh maximum
concentration, μM
C
α4β2W57V
response relative to ACh maximum
concentration, μM
D
α4β2 W57F
response relative to ACh maximum
concentration, μM
E
α4β2 W57Y
response relative to ACh maximum
concentration, μM
ACh
Choline
4OH-GTS-21
AR-R17779

Figure 5

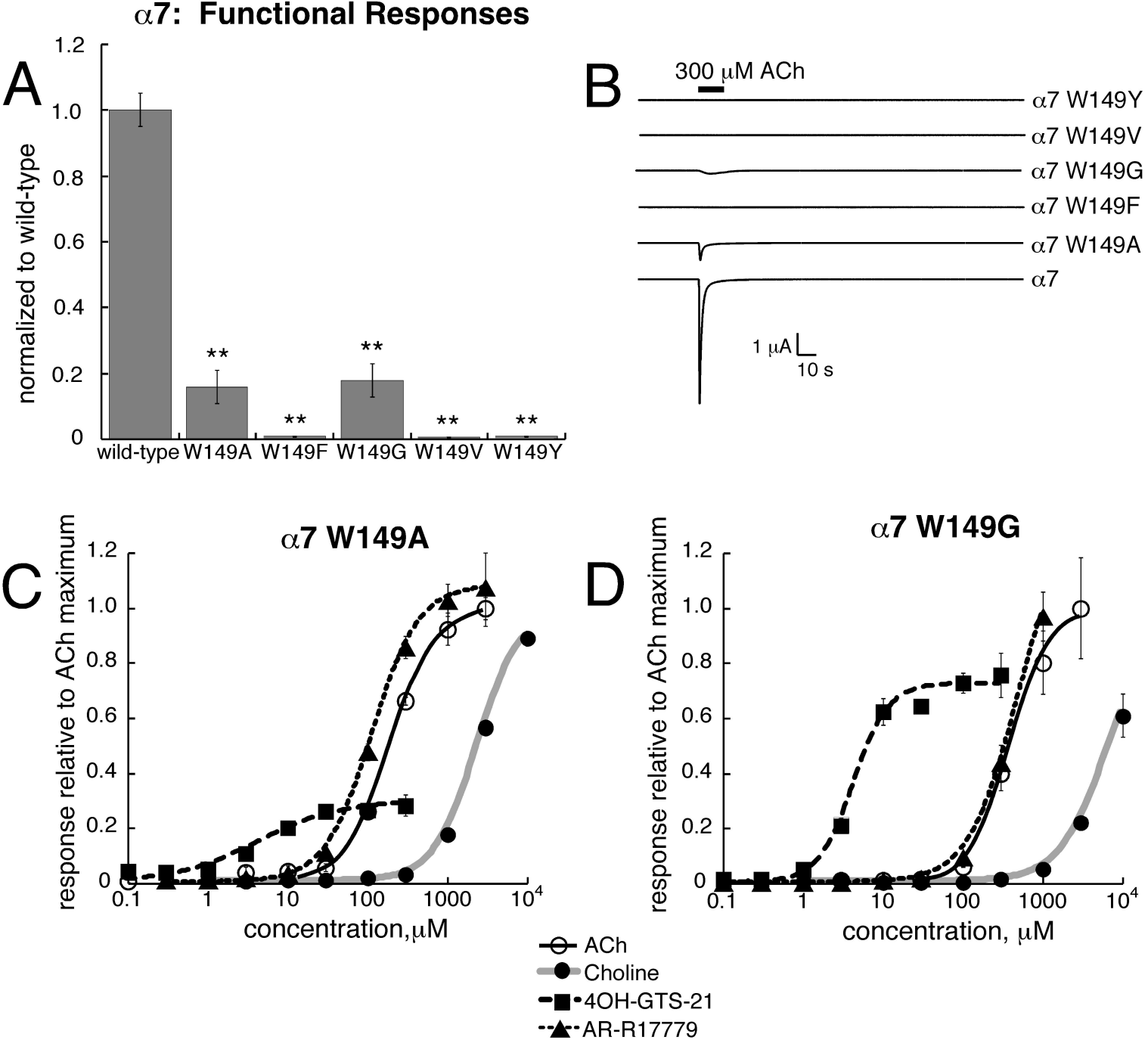
α7: Functional Responses
A
normalized to wild-type
1.2
1.0
0.8
0.6
0.4
0.2
0
**
wild-type
W149A
W149F
W149G
W149V
W149Y
B
300 μM ACh
α7 W149Y
α7 W149V
α7 W149G
α7 W149F
α7 W149A
α7
1 μA
10 s
C
α7 W149A
response relative to ACh maximum
concentration,μM
0.1
1
10
100
1000
10^4
D
α7 W149G
response relative to ACh maximum
concentration, μM
ACh
Choline
4OH-GTS-21
AR-R17779

Figure 6

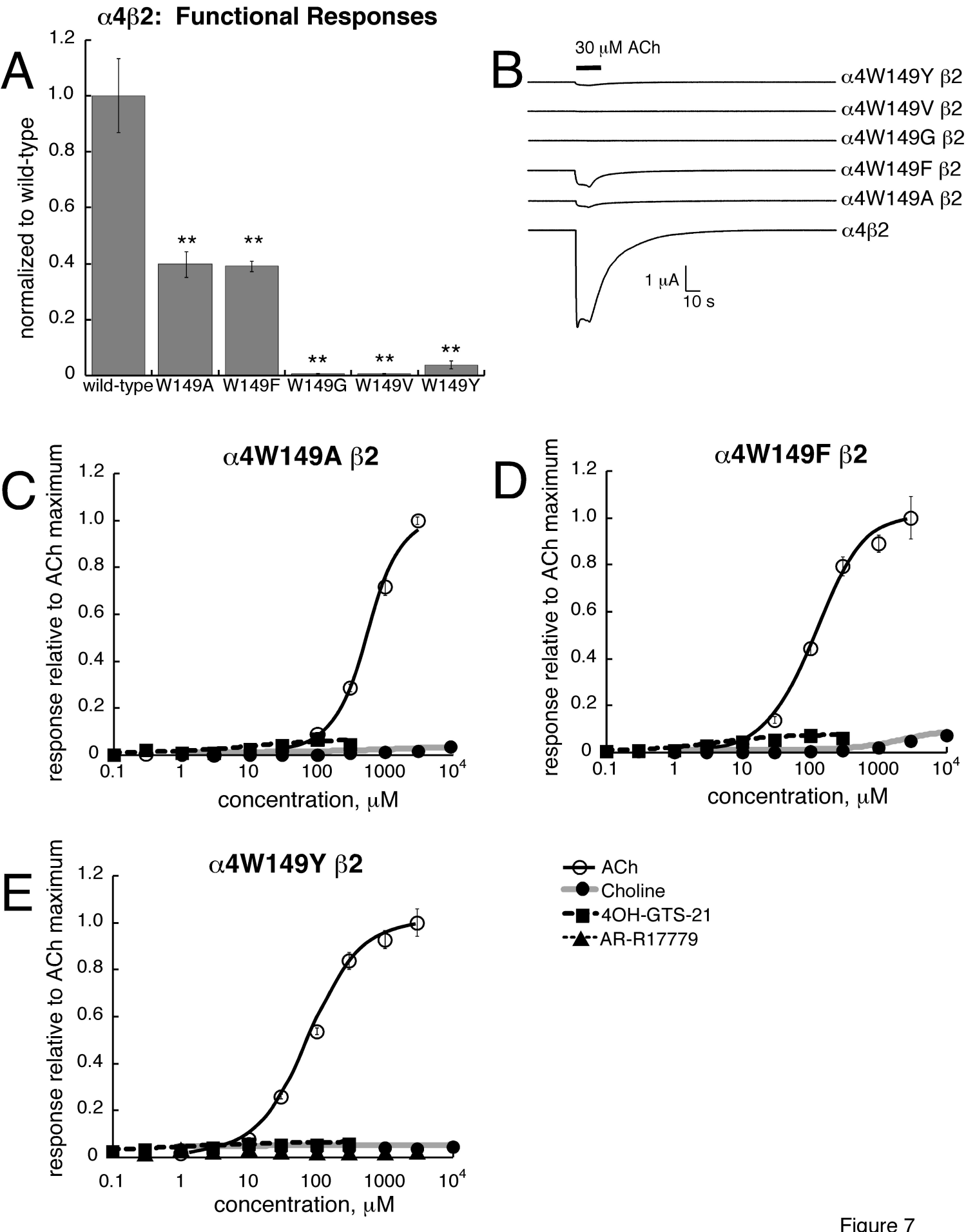
α4β2: Functional Responses
A
normalized to wild-type
1.2
1.0
0.8
0.6
0.4
0.2
0
**
**
**
**
**
wild-type
W149A
W149F
W149G
W149V
W149Y
B
30 μM ACh
α4W149Y β2
α4W149V β2
α4W149G β2
α4W149F β2
α4W149A β2
α4β2
1 μA
10 s
C
α4W149A β2
response relative to ACh maximum
concentration, μM
0.1
1
10
100
1000
10^4
D
α4W149F β2
response relative to ACh maximum
concentration, μM
E
α4W149Y β2
response relative to ACh maximum
concentration, μM
ACh
Choline
4OH-GTS-21
AR-R17779

Figure 7

A

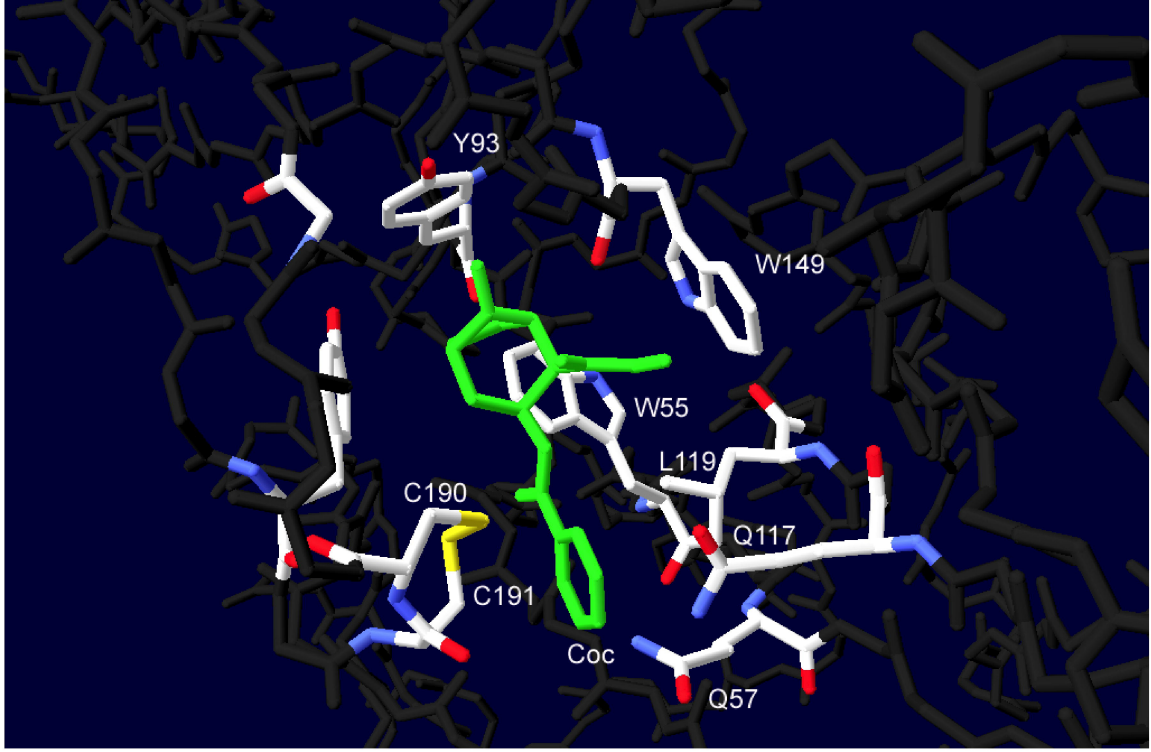
Y93
W149
W55
L119
C190
Q117
C191
Coc
Q57

B

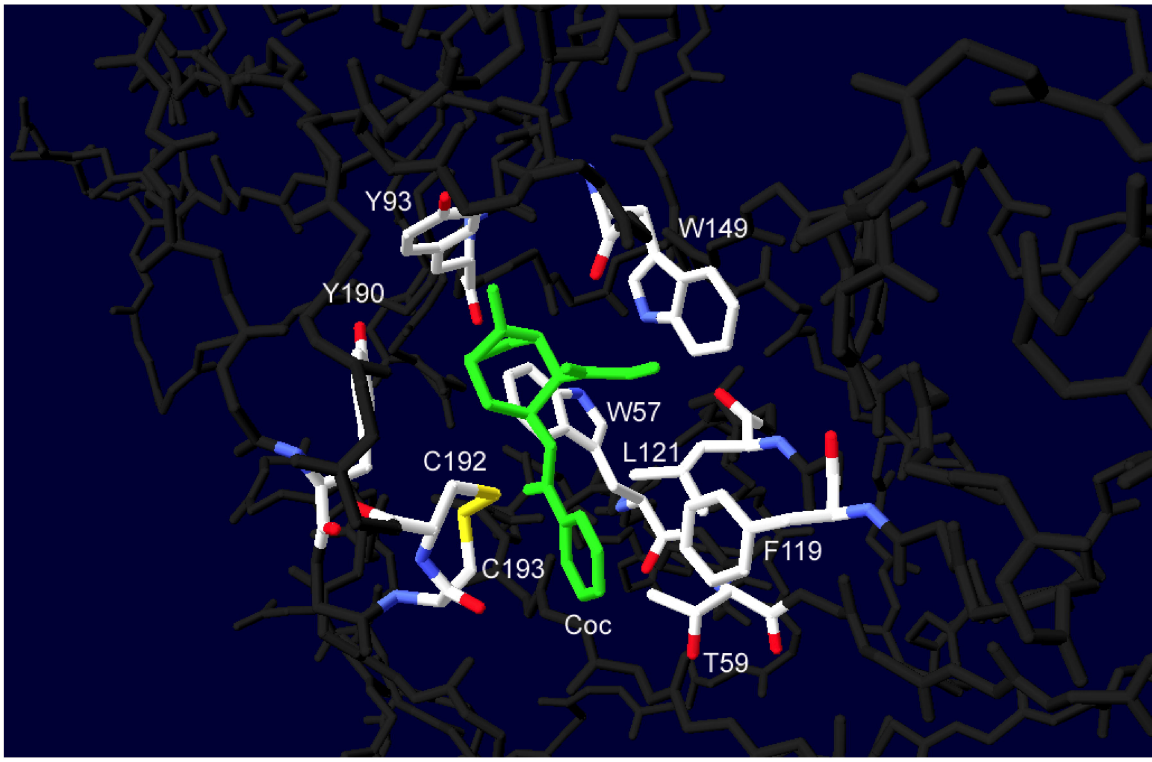
Y93
W149
Y190
W57
L121
C192
F119
C193
Coc
T59

Figure 8

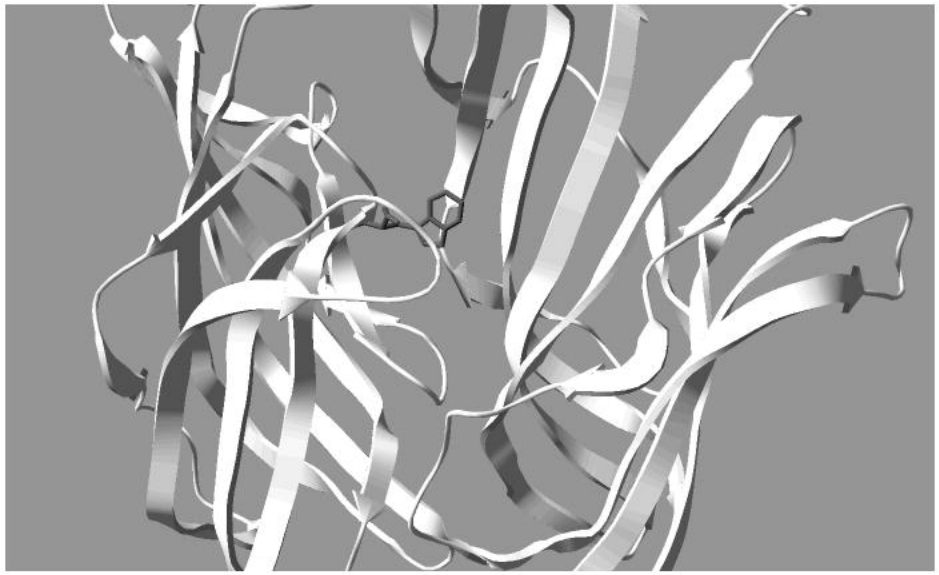

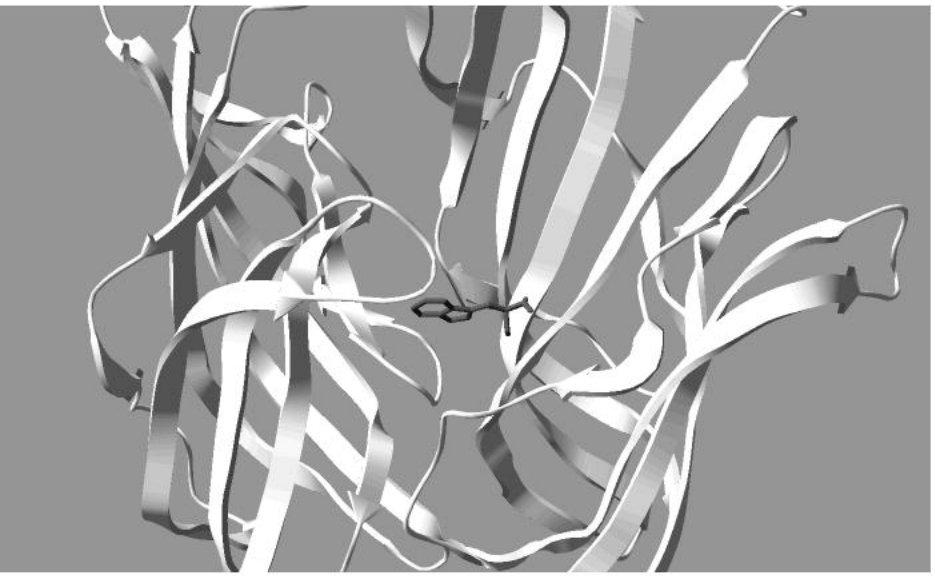

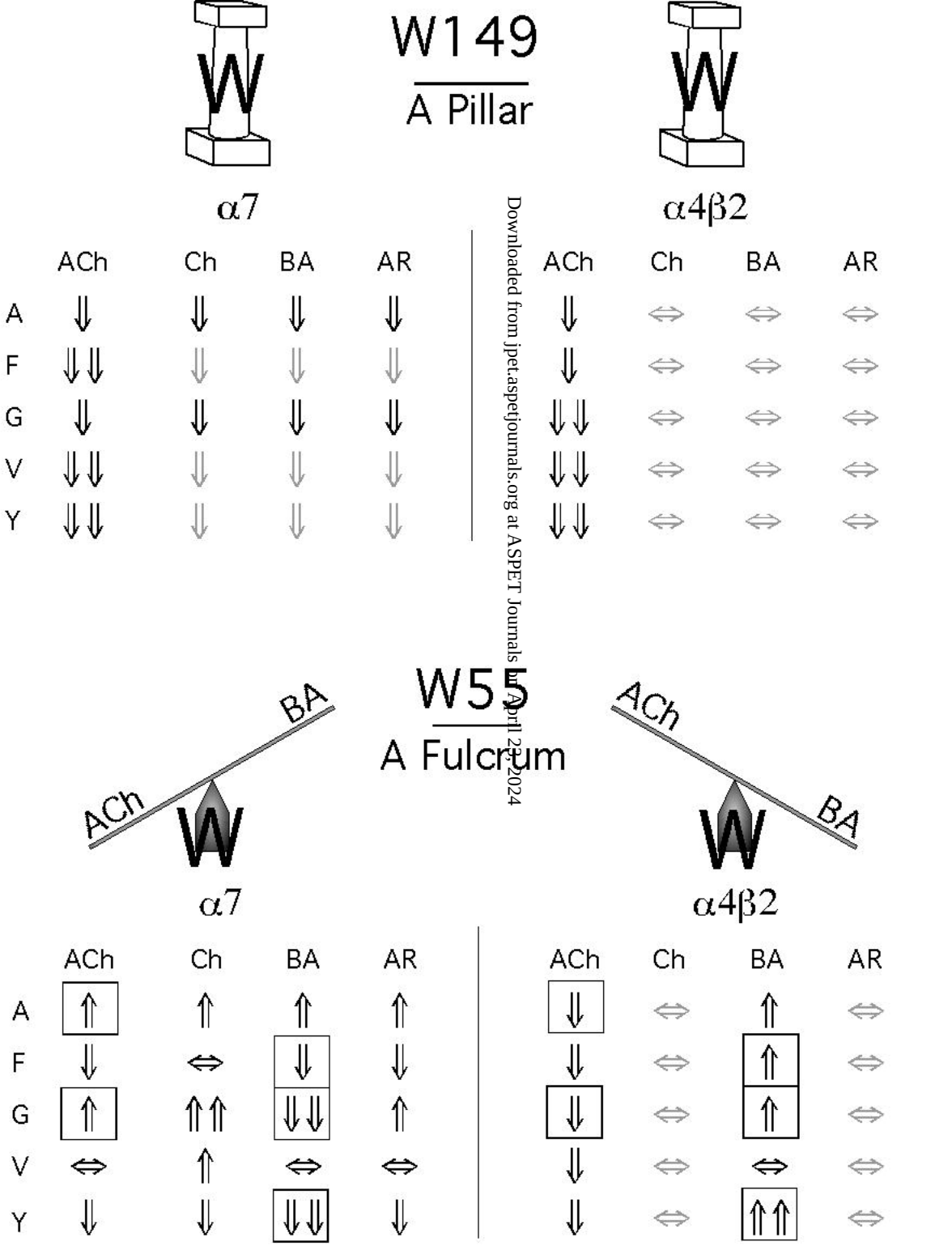

Figure 9